NASA Technical Memorandum 87102

Nonlinear Flap-Lag-Extensional Vibrations of Rotating, Pretwisted, Preconed Beams Including Coriolis Effects

K.B. Subrahmanyam and K.R.V. Kaza
Lewis Research Center
Cleveland, Ohio

(NASA-TM-87102) NONLINEAR FLAP-LAG-EXTENSIONAL VIBRATIONS OF ROTATING, PRETWISTED, PRECONED BEAMS INCLUDING CORIOLIS EFFECTS (NASA) 35 p HC A03/MF A01 CSCL 20K G3/39

N85-34427

Unclas 22230

Prepared for the
19th Midwestern Mechanics Conference
sponsored by The Ohio State University
Columbus, Ohio, September 9-11, 1985

NASA

E-2598

NONLINEAR FLAP-LAG-EXTENSIONAL VIBRATIONS OF ROTATING, PRETWISTED, PRECONED BEAMS INCLUDING CORIOLIS EFFECTS

K.B. Subrahmanyam* and K.R.V. Kaza
National Aeronautics and Space Administration
Lewis Research Center
Cleveland, Ohio 44135

SUMMARY

The effects of pretwist, precone, setting angle, Coriolis forces and second degree geometric nonlinearities on the natural frequencies, steady state deflections and mode shapes of rotating, torsionally rigid, cantilevered beams are studied in this investigation. The governing coupled equations of flap-lag-extensional motion are derived including the effects of large precone (a component of sweep) and retaining geometric nonlinearities up to second degree. The Galerkin method, with nonrotating normal modes, is used for the solution of both steady state nonlinear equations and linear perturbation equations. Parametric results indicating the individual and collective effects of pretwist, precone, Coriolis forces and second degree geometric nonlinearities on the steady state deflections, natural frequencies and mode shapes of rotating blades are presented and discussed. The results indicate that the second degree geometric nonlinear terms, which vanish for zero precone, can produce frequency changes of engineering significance (of the order of 20 percent on the fundamental mode, and about ±4 percent on the second mode). Further confirmation of the validity of including second degree nonlinearities in the analysis is achieved by comparisons of beam theory results to those generated by MSC NASTRAN. The results further indicate that the linear and nonlinear Coriolis effects must be included in analyzing thick blades while these effects can be neglected in analyzing thin blades, typical of advanced turboprop blade configurations. The Coriolis effects are significant on the first flatwise and the first edgewise modes, but are insignificant on higher modes. For those modes where the effect is significant, the linear and nonlinear Coriolis effects oppose one another, the nonlinear effects generally being stronger.

INTRODUCTION

An important phase in the development of advanced turboprop blades, currently in progress at the Lewis Research Center, is the development of analytical blade models that can predict the vibration and flutter characteristics with acceptable accuracy. The turboprop blades are of thin cross sections with large, variable sweep, and are mounted on a rotating hub at a setting angle. Moreover, the blades are subjected to considerable centrifugal loading which causes steady state deflections that are large compared to the blade thickness. It is therefore necessary to include geometric nonlinearities of a sufficient degree, together with other relevant blade complexities in the analysis of turboprop blades.

---

*On leave from NBKR Institute of Science and Technology, Mechanical Engineering Department, Vidyanagar 524413, India and presently Research Associate, University of Toledo, Toledo, Ohio 43606.

Several methods of solution making use of a beam, plate or shell theory are available for the solution of straight, rotating, asymmetric cross section blades (refs. 1 to 3). The coupled equations of motion of such blades based on either linear theory (refs. 4 to 6), or geometric nonlinear theory allowing for small precone (refs. 7 to 9, to mention a few) are available. However, the equations of motion including large variable sweep for blades of advanced turboprop type configurations are not yet available. While finite-element modeling of the turboprop blades appears to be the most appropriate method for blades of such complex geometry, such studies with the existing codes at the Lewis Research Center revealed that the predicted results are satisfactory only for the first few modes. Furthermore, the complicating effects included in the finite element codes, and also in the plate and shell theories, make the understanding of the individual and collective effects of the governing parameters impossible. In order to conduct parametric studies to assess the various complicating effects, and to acquire a physical understanding of the complex blade dynamic problem, it is proposed to use a simpler beam theory to model the rotating blade with the complicating effects successively taken into account to reveal the relative importance of the individual and collective effects. A preliminary study made by using a set of linear equations of motion of a torsionally rigid, pretwisted, rotating blade including Coriolis effects was reported in reference 10 wherein the effects of sweep on the dynamic behavior were introduced by preconing the blade with respect to the plane of rotation. The effects of linear pretwist, precone and linear Coriolis effects on the vibration and stability of rotating blades were discussed in reference 10, and it was pointed out that the Coriolis effects must be included in the analysis of thick blades but could be disregarded in analyzing thin blades possessing small pretwists. The position and width of an instability region was shown to be dependent on the extent of pretwist, precone and whether or not the Coriolis effects were included in the analysis. Although the blade was considered to be torsionally rigid, and hence the results somewhat restricted in generality, considerable information on the various governing parameters was obtained. The first objective of the present effort is to determine the effect of second degree geometric nonlinearities on the natural frequencies, steady state deflections and mode shapes of the blade cases considered in the previous investigation (ref. 10). The second objective is to find the parameter limits within which the second degree geometric nonlinearities are adequate to properly represent the blade dynamic characteristics, by comparison of results produced by beam theory to those produced by MSC NASTRAN. It may be noted here that only the second degree geometric nonlinear effects are included in the present beam theory together with Coriolis effects. Further, there is no restriction on the degree of nonlinearity in the MSC NASTRAN although the Coriolis effects are not accounted by this finite element code. Thus, a fair comparison of frequencies and steady state deflections produced by the present beam theory to those from MSC NASTRAN (for such blade configurations that are insensitive to both linear and nonlinear Coriolis forces) would establish the validity of the restriction of the nonlinearities to only the the second degree. Further complexities of torsional, extensional, rotational and warping couplings can then be addressed once the accuracies of the present restricted beam model are properly validated.

In order to accomplish the stated objectives, the required equations of motion are derived by using the theory presented in reference 9, and by retaining geometric nonlinearities up to second degree. The Galerkin method, with nonrotating normal modes, is employed for the solution of both steady state nonlinear equations and linearized perturbation equations. Parametric studies are conducted to assess the effects of the various terms for configurations representative of propeller blades and advanced turboprop blades. The formulation and solution procedures of the equations of motion are briefly presented in what follows, together with the detailed parametric results and a discussion.

EQUATIONS OF MOTION AND METHOD OF SOLUTION

The coupled flap-lag-extensional equations of motion of a rotating, torsionally rigid, linearly pretwisted and preconed blade of uniform rectangular cross section, shown in figure 1, including Coriolis effects and second degree geometric nonlinearities but disregarding all other higher order effects, can be derived by using the theory presented in references 9 and 11. Such equations are presented below (a list of notation is given in appendix B):

Flatwise bending:

$$m\ddot{w} - m\Omega^2 w \sin^2 \beta_{Pc} + 2m\Omega\dot{v} \sin \beta_{Pc} + m\Omega^2 \sin \beta_{Pc} \cos \beta_{Pc} (x + u - u_F) - (Tw')'$$
$$+ \left\{ w'' (EI_{\eta\eta} \cos^2 \theta + EI_{\xi\xi} \sin^2 \theta) + v''(EI_{\xi\xi} - EI_{\eta\eta}) \sin \theta \cos \theta \right\}'' =$$
$$- \left\{ \Omega^2 \sin \beta_{Pc} \cos \beta_{Pc} \rho (I_{\xi\xi} \sin^2 \theta + I_{\eta\eta} \cos^2 \theta) \right\}' \quad (1)$$

Edgewise bending:

$$m\ddot{v} - m\Omega^2 v + 2m\Omega \cos \beta_{Pc}(\dot{u} - \dot{u}_F) - 2m\Omega\dot{w} \sin \beta_{Pc} - (Tv')'$$
$$+ \left\{ w''(EI_{\xi\xi} - EI_{\eta\eta}) \sin \theta \cos \theta + v''(EI_{\eta\eta} \sin^2 \theta + EI_{\xi\xi} \cos^2 \theta) \right\}'' =$$
$$- \left\{ \Omega^2 \sin \beta_{Pc} \cos \beta_{Pc} \rho (I_{\xi\xi} - I_{\eta\eta}) \sin \theta \cos \theta \right\}' \quad (2)$$

Extension:

$$m[\ddot{u} - \ddot{u}_F - \Omega^2 \cos^2 \beta_{Pc}(u - u_F + x) + w\Omega^2 \sin \beta_{Pc} \cos \beta_{Pc}$$
$$- 2\dot{v}\Omega \cos \beta_{Pc}] - (AEu')' = 0 \quad (3)$$

where

$$T = - \int_x^L m[\ddot{u} - \ddot{u}_F - \Omega^2 (R + x - u_F) \cos^2 \beta_{Pc} - 2\Omega\dot{v} \cos \beta_{Pc}$$
$$+ \Omega^2 w \cos \beta_{Pc} \sin \beta_{Pc}]dx, \quad (4)$$

$$u_F = \frac{1}{2} \int_0^x (v'^2 + w'^2) dx, \tag{5}$$

and

$$m = \iint \rho dy\, dz,\ A = \iint dy\, dz,\ I_{\xi\xi} = \iint y^2\, dy\, dz,\ I_{\eta\eta} = \iint z^2\, dy\, dz,$$

$$(\ )' = \frac{\partial}{\partial x}(\ ),\ (\dot{\ }) = \frac{\partial}{\partial t}(\ ) \tag{6}$$

Defining the following parameters,

$$\bar{w} = w/L,\ \bar{v} = v/L,\ \eta = x/L,\ \tau = \Omega t,\ \bar{R} = R/L, \text{ etc.}, \tag{7}$$

assuming solutions are separable in time and space, and making note of the following relations

$$\frac{d}{dx} = \frac{d}{d\eta} \cdot \frac{d\eta}{dx} = \frac{1}{L}\frac{d}{d\eta},\ \frac{d}{dt} = \Omega \frac{d}{d\tau} \text{ etc.}, \tag{8}$$

one can rewrite equations (1) to (3) in the following nondimensional forms:

$$\ddot{\bar{w}} + 2 \sin \beta_{Pc} \dot{\bar{v}} - \bar{w} \sin^2 \beta_{Pc} - \frac{1}{2} \sin \beta_{Pc} \cos \beta_{Pc} \int_0^\eta (\bar{v}'^2 + \bar{w}'^2) d\eta$$

$$- \cos^2 \beta_{Pc} (\bar{w}'' Q - \bar{w}' S) - 2 \cos \beta_{Pc} \left[\bar{w}'' \int_\eta^1 \dot{\bar{v}}\, d\eta - \bar{w}' \dot{\bar{v}} \right]$$

$$+ \sin \beta_{Pc} \cos \beta_{Pc} \left[\bar{w}'' \int_\eta^1 \bar{w}\, d\eta - \bar{w}' \bar{w} \right] + \xi \bar{w}^{iv} \left(\cos^2 \theta + \frac{b^2}{d^2} \sin^2 \theta \right)$$

$$+ \bar{w}'''(2\gamma\xi \sin 2\theta)\left(\frac{b^2}{d^2} - 1\right) + \bar{w}''(2\gamma^2\xi \cos 2\theta)\left(\frac{b^2}{d^2} - 1\right) + \xi \bar{v}^{iv}\left(\frac{1}{2} \sin 2\theta\right)\left(\frac{b^2}{d^2} - 1\right)$$

$$+ \bar{v}'''(2\gamma\xi \cos 2\theta)\left(\frac{b^2}{d^2} - 1\right) - \bar{v}''(2\gamma^2\xi \sin 2\theta)\left(\frac{b^2}{d^2} - 1\right) + \sin \beta_{Pc} \cos \beta_{Pc} \bar{u}$$

$$+ \bar{w}'' \int_\eta^1 \ddot{\bar{u}}\, d\eta - \bar{w}'' \int_\eta^1 \bar{u} \cos^2 \beta_{Pc}\, d\eta - \bar{w}' \ddot{\bar{u}} + \bar{w}' \bar{u} \cos^2 \beta_{Pc}$$

$$= -\eta \sin \beta_{Pc} \cos \beta_{Pc} - \frac{I_{\eta\eta}\gamma}{AL^2}\left(\frac{b^2}{d^2} - 1\right) \sin \beta_{Pc} \cos \beta_{Pc} \sin 2\theta \tag{9}$$

$$\ddot{\bar v} - 2\sin\beta_{Pc}\,\dot{\bar w} - \bar v - \cos^2\beta_{Pc}(\bar v''Q - \bar v'S) - 2\cos\beta_{Pc}\left[\bar v''\int_\eta^1 \dot{\bar v}\,d\eta - \bar v'\dot{\bar v}\right]$$

$$- \cos\beta_{Pc}\frac{d}{d\tau}\int_0^\eta (\bar v'^2 + \bar w'^2)\,d\eta + \sin\beta_{Pc}\cos\beta_{Pc}\left[\bar v''\int_\eta^1 \bar w\,d\eta - \bar v'\bar w\right]$$

$$+ \bar w^{iv}\xi\left(\frac{1}{2}\sin 2\theta\right)\left(\frac{b^2}{d^2} - 1\right) + \bar w'''(2\gamma\xi\cos 2\theta)\left(\frac{b^2}{d^2} - 1\right)$$

$$- \bar w''(2\gamma^2\xi\sin 2\theta)\left(\frac{b^2}{d^2} - 1\right) + \bar v^{iv}\xi\left(\sin^2\theta + \frac{b^2}{d^2}\cos^2\theta\right) - \bar v'''(2\gamma\xi\sin 2\theta)\left(\frac{b^2}{d^2} - 1\right)$$

$$- \bar v''(2\gamma^2\xi\cos 2\theta)\left(\frac{b^2}{d^2} - 1\right) + 2\cos\beta_{Pc}\dot{\bar u} - \bar v''\int_\eta^1 \bar u\cos^2\beta_{Pc}\,d\eta$$

$$+ \bar v''\int_\eta^1 \ddot{\bar u}\,d\eta - \bar v'\ddot{\bar u} + \bar v'\bar u\cos^2\beta_{Pc} = -\sin\beta_{Pc}\cos\beta_{Pc}\left(\frac{I_{\eta\eta}\gamma}{AL^2}\right)\cos 2\theta \qquad (10)$$

$$\ddot{\bar u} - \left[\frac{d^2}{d\tau^2}\,\frac{1}{2}\int_0^\eta (\bar v'^2 + \bar w'^2)\,d\eta\right] - \cos^2\beta_{Pc}\bar u + \frac{1}{2}\cos^2\beta_{Pc}\int_0^\eta (\bar v'^2 + \bar w'^2)\,d\eta$$

$$+ \bar w\sin\beta_{Pc}\cos\beta_{Pc} - 2\dot{\bar v}\cos\beta_{Pc} - (AE/m\Omega^2L^2)\bar u'' = \eta\cos^2\beta_{Pc} \qquad (11)$$

where

$$Q = \bar R(1 - \eta) + 0.5\left(1 - \eta^2\right),\ S = (h + \eta),\ (\bar w)' = \frac{d}{d\eta}(\bar w),\ (\dot{\bar w}) = \frac{d}{d\tau}(\bar w),$$

$$\xi = (EI_{\eta\eta}/\rho AL^4\Omega^2),\ \text{and}\ \theta = \varphi + \gamma\eta \qquad (12)$$

Before discussing the method of solution, it is worthwhile to point out the various important linear terms associated with precone, and also the nonlinear terms existing in the present equations. The linear terms associated with precone are addressed first. Referring to equation (9), one can see that a linear softening term, ($-\bar w\sin^2\beta_{Pc}$), appears in the flap equation. This term vanishes for zero precone, but becomes an important term for suitably large values of precone and rotational speeds, and contributes to the mechanism of rotation induced instability. Next, the terms ($2\sin\beta_{Pc}\dot{\bar v}$) and ($-2\sin\beta_{Pc}\dot{\bar w}$) in equations (9) and (10) respectively are the linear Coriolis force terms that arise due to the inclusion of precone. The effect of these terms on the linear frequencies has been discussed in detail in reference 10. Considering equation (11), one observes that there is one linear term ($\bar w\sin\beta_{Pc}\cos\beta_{Pc}$) which vanishes for zero precone, and that the linear Coriolis force term ($2\dot{\bar v}\cos\beta_{Pc}$) appears in this equation whether or not precone is present in the derivation of the equations. Since it will be shown that the inclusion of extensional degree of freedom is not that important for analyzing both thin and thick blades, further discussion of the other nonlinear terms associated with the extensional deformation will not be attempted in this section. Next the important nonlinear terms existing in equations (9) and (10) are considered. The nonlinear Coriolis force terms are shown by underlining them once, and these terms will be present in the equations even when precone is absent. The nonlinear terms which are shown by underscoring them twice in equations (9) and (10) are the contributions from the tension terms (Tw')' and (Tv')', as are two of the three nonlinear Coriolis terms just discussed. However, the doubly underlined terms vanish for zero precone. Finally, the term shown by broken underlining is the effect of foreshortening of the blade. This term also vanishes for zero precone. It may also be mentioned here that for the limiting case value of 90° precone, all nonlinear terms in equations (9) to (11) vanish excepting those associated with extensional inertia ($\ddot{u}$, $\ddot{u}_F$). Since the nonlinear terms associated with extensional deformation are already noted to be unimportant, the effect of geometric nonlinearities should become almost negligible at $\beta_{pc} = 90°$.

The flap-lag-extensional equations are solved by the Galerkin method by assuming that the dimensionless bending and extensional deflections in terms of a series of generalized coordinates and mode shape functions are as follows:

$$\bar{w} = \sum_j (w_{oj} + \Delta w_j(\tau))\Psi_j(\eta) \tag{13}$$

$$\bar{v} = \sum_j (v_{oj} + \Delta v_j(\tau))\Psi_j(\eta) \tag{14}$$

$$\bar{u} = \sum_j (u_{oj} + \Delta u_j(\tau))\theta_j(\eta) \tag{15}$$

where

$$\Psi_j(\eta) = \cosh(\beta_j\eta) - \cos(\beta_j\eta) - \alpha_j[\sinh(\beta_j\eta) - \sin(\beta_j\eta)] \tag{16}$$

$$\theta_j(\eta) = 2\sin(\gamma_j\eta) \tag{17}$$

$$\gamma_j = \pi(j - \tfrac{1}{2}) \tag{18}$$

Equations (16) to (18) are the nonrotating normal modes for a cantilevered beam fixed at $\eta = 0$, and free at $\eta = 1$. Furthermore, the quantities w_{oj}, v_{oj} and u_{oj} in the generalized coordinates constitute the equilibrium quantities while Δw_j, Δv_j and Δu_j are the perturbation quantities.

By substituting only the steady state equilibrium quantities into the nonlinear equations (9) to (11), assuming n-normal modes for each of the variables $\bar{u}$, $\bar{v}$, and $\bar{w}$ and carrying out the Galerkin process traditionally, one obtains a set of 3n nonlinear equations in terms of w_{oj}, v_{oj} and u_{oj}. The constants α_j and β_j are taken from reference 12, and the resulting equilibrium equations are solved by using a computer program based upon a finite-difference Levenberg-Marquardt algorithm (ref. 13). Next, equations (13) to (15) are substituted into equations (9) to (11), the Galerkin process is carried out again, the equilibrium equations are subtracted from the result, and all nonlinear quantities in the perturbation parameters are discarded to obtain the linear perturbation equations (expressed in terms of the equilibrium generalized coordinates) that define the unsteady blade motion about the equilibrium operating condition. The steady state equilibrium equations, and the linear perturbation equations are written in the following matrix notations:

$$[\underset{\sim}{L}]\{X_0\} + [\underset{\sim}{NL}]\{X_0\} = \{B\} \tag{19}$$

$$[\underset{\sim}{M}]\{\ddot{X}\} + [\underset{\sim}{C}]\{\dot{X}\} + [\underset{\sim}{K}]\{X\} = 0 \tag{20}$$

where

$$X_0 = \{w_{o1}, w_{o2}, \ldots, w_{on}, v_{o1}, v_{o2}, \ldots, v_{on}, u_{o1}, u_{o2}, \ldots, u_{on}\}^T, \tag{21}$$

$$X = \{\Delta w_1, \Delta w_2, \ldots, \Delta w_n, \Delta v_1, \Delta v_2, \ldots, \Delta v_n, \Delta u_1, \Delta u_2, \ldots, \Delta u_n,\}^T, \tag{22}$$

with $\underset{\sim}{L}$ and $\underset{\sim}{LN}$ being respectively the linear and nonlinear parts of the equilibrium equations, and $\underset{\sim}{M}$, $\underset{\sim}{C}$, and $\underset{\sim}{K}$ being the mass, Coriolis and stiffness matrices respectively. Elements of these matrices are presented in appendix A. Equation (20) is transformed into an eigenvalue problem, integrations are performed using a Gaussian quadrature formula, and the steady state deflections, eigenvalues and eigenvectors are determined for various cases of rotating blades.

RESULTS AND DISCUSSION

The nonlinear steady state equations (19), and the eigenvalue problem that results from the transformation of equation (20) were solved by using computer programs developed in FORTRAN language. The general computer program developed for the solution of equation (20) gives the natural frequencies per unit rotational speed, (p/Ω). In the presence of Coriolis effects, the frequencies will occur in pairs of purely imaginary quantities for a conservative system. In the absence of Coriolis effects, the frequency equation (20) reduces to a standard eigenvalue problem, the eigenvalues of which are real quantities of (p^2/Ω^2). Thus, specialized simple cases were solved by modifying the general computer program. Typical thickness ratios which approximately represent advanced turboprop blades (d/b = 0.05) or propeller blades (d/b = 0.25) were considered for aspect ratios of the order of 5 to 10. It may be noted that the radius of the disc, R, is assumed to be zero for simplicity.

Convergence

The convergence of solutions produced by the Galerkin method for the coupled flap-lag-extension equations, using various numbers of nonrotating normal modes for the independent variables, is shown in table I. The blade considered for this convergence study has a precone of 30° and a thickness ratio of 0.5. The blade chord at the root is set perpendicular to the axis of rotation ($\varphi = 0°$) and the blade rotational speed is one half of the fundamental mode frequency of the same nonrotating blade ($\Omega/\omega_1 = 0.5$). Natural frequencies for this blade with zero pretwist are determined by varying the number of nonrotating normal modes, n, used in the series solution assumed. It can be seen from this table that a five-mode solution produces the frequencies of the linear equations, and also those from a perturbation solution of the nonlinear equations, converged to five significant figures. A further comparison of the present flap-lag-extension frequencies, (p/λ_1), obtained from the solution of the linear equations to those given in references 10 and 14 shows an excellent agreement. Further results for various combinations of pretwist, precone, setting angle and rotational speed are obtained by using a five-mode Galerkin solution, and the individual and collective effects of the various parameters are discussed in the following sections. The validity of restricting the geometric nonlinearities to second degree only is assessed by comparison of the present beam theory results to those produced by MSC NASTRAN for specialized cases of thin blades in the following section.

Comparison of Present Results

Comparison of the frequencies from the solution of the present linear equations and those from a perturbation solution of the nonlinear equations is made to the frequencies produced by MSC NASTRAN using 250 CQUAD4 elements in tables II to IV for typical values of precone, rotational speed and thickness ratio. The steady state equilibrium deflections produced by the present beam theory and those produced by MSC NASTRAN are compared in figure 2. Considering the results presented in table II corresponding to a thin blade possessing zero pretwist, zero precone and zero setting angle, one can see that the lowest six-mode frequencies obtained from perturbation solution of the beam theory equations agree to within one half of 1 percent with those given by MSC NASTRAN, for wide range of rotational speeds. It may be noted that the present flap-lag-extensional equations cannot predict the torsional frequencies since this degree of freedom is not considered in this study. Next, a comparison of the lowest three frequencies of the same blade considered earlier but with a 15° precone are presented in table III. A further comparison of linear and nonlinear frequencies is also made in this table. Here also, the agreement between the two sets of results is good. The effect of geometric nonlinearities on the lowest three flatwise modes is seen to be of a stiffening character, and the frequencies are found to increase with increasing rotational speeds due to the nonlinearities. Table IV shows further comparison of results for large values of precone, for both thin and thick blade cases, at various rotational speeds. Considering the trend of results observed so far for thin blades, it is evident that the first bending modes in both flatwise and edgewise directions are affected much more than higher modes. The percent difference between beam theory results and MSC NASTRAN results increases with increasing precone for a given rotational speed, and for a given precone with increasing rotational speeds. However, for practical rotor speeds of the order of $(\Omega/\omega_1) \leq 1$, the difference between the two sets of results is not greater than 5 percent. When a comparison of the results obtained for thick blades ($d/b = 0.25$), is made, it appears that the percent error observed for the second mode is quite large. In order to assess the effect of ignoring the Coriolis effects, results for the thick blade cases are also obtained from the present beam theory by ignoring the Coriolis effects, and these results are compared to the corresponding ones from MSC NASTRAN. These are also included in table IV. From this comparison of results, it is evident that the results from MSC NASTRAN are in closer agreement with the corresponding results from the beam theory when the Coriolis effects are ignored in beam theory. It should be noted here that the rather large difference observed for the second mode frequency of thick blades, (which is the fundamental edgewise frequency), may be partially attributed to the fact that the present slender beam approximation in the beam theory may be inadequate to predict the frequencies of stubby blades in general and the stiff edgewise mode frequencies in particular. Proper comparisons of these frequencies is only possible by including the shear and rotary inertia effects in both beam theory and MSC NASTRAN.

Next, the steady state deflections for thin blades given by the present beam theory are considered. For the untwisted blade cases considered in this work for various precones and rotational speeds, it is observed that the flatwise deflection is the most significant while the edgewise and extensional deflections were almost insignificant. The extensional deformation was found to be more significant than the edgewise deflection. However, for pretwisted blades, both flatwise and edgewise steady state deflections became quite significant, and the magnitudes of these deflections were found to be large in comparison to the corresponding untwisted blade deflections. Thus, for the untwisted, thin blade cases, the distribution of dimensionless flatwise deflection, $\overline{w}$, along the length of the blade obtained from the present beam theory is compared to the corresponding one from MSC NASTRAN in figures 2(a) to (d), for typical precones and rotational speeds. An examination of these results indicates that the trends shown by both sets of results considered are consistent. Furthermore, the agreement between the two sets of results is extremely close for low rotational speeds. The difference between beam theory results and MSC NASTRAN gradually increased from zero at the root section to the maximum at the tip in general. For precones of the order of 45° and rotational speed parameter value of up to $(\Omega/\omega_1) = 1.0$, the greatest difference between the two sets of results, (steady state deflections and frequencies up to third mode), has been found to be of the order of 5 percent for thin blades. It is interesting to note that the deflections given by the beam theory are consistently greater than those produced by MSC NASTRAN.

From the foregoing discussion of results, it appears that the present beam theory, including geometric nonlinearities up to second degree only, predicts the natural frequencies and steady state deflections to an acceptable degree of accuracy in the case of thin blades having precones of up to 45° and for blade rotational speeds that are practically encountered in their applications. It is believed that the inclusion of the torsional degree of freedom, which is necessary for calculation of stability boundaries for the blades, should not alter this trend of agreement of results, since the torsional mode coupling may affect the stability boundary but not the convergence of the first few modes that are well separated from the basic torsional mode frequency. It may thus be concluded that the second degree nonlinearities are adequate for modeling thin blades with large precone and for rotational speeds encountered in their practical operational range.

INDIVIDUAL AND COLLECTIVE EFFECTS

In order to understand the individual and combined effects of precone, linear and nonlinear Coriolis forces, various nonlinear terms (second degree geometric nonlinearities) and pretwist on the frequencies of rotating blades, parametric studies were conducted for two typical thickness ratios of [illegible] 0.25 for various setting angles (collective pitch). These results are presented in tables V to IX. Figure 3 shows the effect of setting angle, pretwist and precone variations on the fundamental mode frequency parameter, (p_1/λ_1).

Effect of Varying Precone

In order to determine the effect of varying precone on the frequency parameter ratios of untwisted blades with zero setting angle ($\varphi = 0$), the flap-lag-extension equations were solved for a typical rotational parameter value of $(\Omega/\omega_1) = 1.0$. The value of precone was changed from 10° to 50°, and the linear and nonlinear frequencies were determined which include the Coriolis effect terms also. These frequencies are listed in table V together with the percent frequency variation based upon the nonlinear frequency for each mode. The following observations are made from the results presented in table V.

1. For a given rotational speed and thickness ratio, the flatwise mode frequencies decrease with increasing precone in the case of both linear and nonlinear theories. The first edgewise mode frequency, (refer the second mode frequency of thick blade with $d/b = 0.25$), given by linear equations or nonlinear equations shows an increasing trend with increasing precone.

2. The flatwise mode frequencies produced from the perturbation solution of the nonlinear equations are higher than the corresponding frequencies obtained from the linear set of equations. The fundamental edgewise frequency given by the solution of nonlinear equations is lower than the corresponding linear solution value.

3. The effect of geometric nonlinearities, as could be seen from the percent frequency variation, increases with increasing precones of up to 50° considered here. The frequency change for flatwise modes is seen to be positive (stiffening) while for edgewise modes it is negative (softening). However, it should be noted that for 90° precone, the effect of geometric nonlinearities becomes almost zero as should be expected.

4. The fundamental mode frequency shows the strongest frequency variation (positive for flatwise mode and negative for edgewise mode) due to the presence of nonlinearities, and this effect is seen to decrease as the mode number is increased.

Effects of Pretwist, Coriolis Forces and Geometric Nonlinearities

The individual and combined effects of pretwist, precone, Coriolis forces and thickness ratio on the frequencies of rotating blades in the absence of geometric nonlinearities were presented and discussed in reference 10. However, the linear frequencies are presented again in all the following tables for the purpose of completeness, and also to provide an easy access for discussing all the results together. The slight differences (at the fourth significant figure) one may find between the linear frequencies presented in this paper and those in reference 10 are due to the fact that the extensional degree of freedom was ignored in reference 10 while this degree of freedom is included in this work, and also due to the fact that the methods of solution used in these two works are different.

In order to ascertain the individual and combined effects of precone, rotational speed, Coriolis forces and the various terms that arise in the equations due to the inclusion of second degree geometric nonlinearities, several cases rotating blades were solved. These results are presented in tables VI and VII for both untwisted and 30° pretwisted blades having zero collective pitch ($\varphi = 0°$). Typical rotational parameter values of (Ω/ω_1) = 0.5, 0.8 and 1.0 were considered in this study since these values generally encompass the practical operational speeds of advanced turboprop blades. The frequency parameter ratios (p/λ_1) obtained from the solution of the linear equations, including or excluding the Coriolis effects, are presented first in these tables. Next, the frequencies obtained from the perturbation solution of the nonlinear equations are presented, starting with the frequencies of full nonlinear equations followed by those obtained by ignoring one key parameter in the nonlinear equations at one time. Thus, the frequency parameters under the column with $A_{ijk} = 0$ represent the frequencies obtained by ignoring the foreshortening effects although all other effects are present, those under the column with ($D_{ijk} = 0$, $E_{ijk} = 0$) illustrate the effect of ignoring the nonlinear terms arising from the centrifugal tension terms ($(Tw')'$ and $(Tv')'$), while the frequencies in the last column indicate the effect of ignoring the nonlinear terms associated with the extensional deformation together with those from centrifugal tensions. While the results presented in this form are useful for future comparison, the individual effects will be clearer if percent variation of the frequencies are calculated for each category based on full nonlinear solutions. This is accomplished in tables VIII and IX. The following observations can be made from the results presented in these tables:

1. The limiting values of precone of zero and 90° are considered first on the vibrational characteristics. When $\beta_{PC} = 0$, one can see from equations (9) to (10) that the flap-lag equations are coupled through the nonlinear Coriolis force terms together with the linear and nonlinear extensional deformation coupling terms. Coupling due to the latter category of terms is not that important however. Pretwist in the blade brings in the additional important structural coupling between flap and lag deflections. Thus, for untwisted and pretwisted blades, the effects of geometric nonlinearities (excepting for the Coriolis terms which are important for thick blades) on the natural frequencies is almost negligible when precone is zero. When the precone is 90°, the flap and the lag equations are coupled through linear Coriolis force terms and extensional inertia even for the untwisted case, while the extensional equation of motion is coupled through the inertia associated with foreshortening. Since the right hand side for this case of 90° precone is zero for all the coupled equations, the steady state deformations will be absent, and the equations produce results that depend only on Coriolis effects. This can be verified from the results presented in table VI(a) for 90° precone case. The effects of geometric nonlinearities and linear and nonlinear Coriolis forces are therefore important for precone angles other than these extremes.

2. Although the frequencies show both increasing and decreasing trends for a given precone with an increase in rotational speed, (refer to table VI(a)), the effect of geometric nonlinearities is seen to increase the frequencies of

flatwise modes, and to decrease the frequency of first edgewise mode (refer tables VIII and IX) for untwisted and pretwisted blades for the practical rotor speeds considered.

3. The effect of second degree geometric nonlinearities is the greatest on the fundamental mode, and decreases as the mode number is increased. The effect of second degree geometric nonlinearities increases as the rotational speed is increased. By referring to tables VII(a) and (b), it can also be seen that an increase in precone from 15° to 45° increases the effect of the geometric nonlinear terms considerably for a given rotational speed.

4. In tables VIII and IX, the percent frequency variation due to the absence of linear or nonlinear Coriolis effect terms in the presence the other and with second degree geometric nonlinearities is presented. These frequency variations are calculated based upon full nonlinear frequencies. It can be seen from these results that the nonlinear Coriolis effects are stronger than the linear ones in affecting the frequencies of all modes for high rotational speeds generally. Both hardening and softening characteristics are exhibited by the linear and nonlinear Coriolis terms for a given mode with increasing rotational speed. This trend is to be attributed to the fact that even though the linear (or nonlinear) Coriolis terms are ignored and nonlinear (or linear) Coriolis terms are retained in the equations, the presence of other geometric nonlinearities also affect the resulting frequencies which causes these mixed trends. It emerges clearly, however, that both linear and nonlinear Coriolis effects are important for high thickness ratio untwisted or pretwisted blades, and these effects are insignificant for low thickness ratio blades. For the cases where the Coriolis effects are important, the linear Coriolis effects oppose the nonlinear Coriolis effects. The influence of the linear and nonlinear Coriolis effects are the greatest on the first flatwise mode and on the first edgewise mode, and are insignificant on other higher modes. These effects are more pronounced for larger precones and higher rotational speeds. One may thus conclude that both linear and nonlinear Coriolis effects can be ignored in analyzing thin blades which are typical of advanced turboprop blade configurations.

5. The effects of ignoring either the foreshortening terms, or the centrifugal tension coupling terms on the nonlinear frequencies are shown in the last two columns of tables VIII and IX. It can be seen from these results that these two effects produce the greatest variations on the frequencies, and that the first mode is affected to the greatest extent. It may also be noted that these terms arise due to the presence of precone, and the frequency increases by nearly 20 percent due to the presence of the second degree geometric nonlinear terms.

6. The onset of static instability for various cases of preconed rotating blades with and without pretwist was predicted by using the linear equations in reference 10. It was shown that a 60° preconed blade with a thickness ratio of 0.05 becomes statically unstable for $1.48 \leq (\Omega/\omega_1) \leq 1.49$ if linear equations including Coriolis effects were used for the prediction of the instability. By using the present second degree geometric nonlinear equations with Coriolis effects, this instability was found to occur for $1.13 \leq (\Omega/\omega_1) \leq 1.14$ for an untwisted blade, and for a 30° pretwisted blade. When the untwisted thin blade with 60° precone was solved by using MSC NASTRAN, it was observed that the pseudo-static configuration became unstable at $(\Omega/\omega_1) = 0.8$. Since the results from the analysis using MSC NASTRAN gave consistently good

agreement of frequencies up to the lowest three modes with the corresponding ones from the present beam theory including second degree geometric nonlinearities, it is believed that the torsional coupling (which is present in MSC NASTRAN analysis but absent in beam theory) must have been responsible for predicting a lower instability value. It thus appears that the torsional coupling must be included in the beam theory for a fair prediction of instability boundaries.

7. The effect of pretwist in coupling the modes of preconed rotating blades was studied in reference 10. Similar conclusions are valid here also since the second degree geometric nonlinearities and the nonlinear Coriolis effects have not affected the higher modes to any great extent as to alter the coupling trends for thin blades. The well established coupling trend of decreasing the lower frequency (first edgewise mode frequency) and increasing the higher frequency (second flatwise mode frequency) of the two closer modes of untwisted blade due to pretwisting is evident in the results presented in tables VIII(a) and (b) for the thick blade case, for the precones and rotational speeds considered. The effects of second degree geometric nonlinearities and Coriolis forces on the frequencies of pretwisted blades are similar to those observed for untwisted blade cases.

8. Frequency parameter ratios for 90° setting angle were also determined from the present linear and nonlinear equations. It was found that for a thin blade (d/b = 0.05), having β_{pc} = 45° and (Ω/ω_1) = 1.0, the nonlinear frequencies of the lowest three modes were greater than the respective linear frequencies by about 0.067, 0.005 and 0.002 percent. These frequency variations for a thick blade (d/b = 0.25) were of the order of 1.979, -0.263 and 0.137 percent respectively. By comparing these results with those obtained for the zero setting anlge case (φ = 0°) presented in table VIII(b), one can conclude that the effects of geometric nonlinearities are far more severe for φ = 0° than for φ = 90°. Results pertaining to φ = 90° for pretwisted blades also show similar trends to those observed for the untwisted case discussed above. For brevity these results are not presented. Since it has been established that the geometric nonlinearities and Coriolis forces affect the fundamental mode most severely, it is felt desirable to present the variation of the fundamental mode frequency parameter ratio with respect to the variation of precone for various combinations of setting angle and pretwist. This is shown in figure 3. It can be seen from this figure that for a given rotational speed and precone, the variation of pretwist changes the fundamental mode frequency to an appreciable extent for setting angle φ of around 45°. While the fundamental mode frequency is quite distinct and well separated for each combination of setting angle and pretwist at zero degree precone, these frequency values droop down to a small zone at 90° precone. Since for β_{pc} = 90°, the preconed blade becomes a cantilevered shaft, the effect of setting angle vanishes, and the slight difference observed in the frequency values must be attributed to the coupling effects arising from pretwist and the linear Coriolis terms. Finally, results were obtained for the various cases discussed earlier by ignoring the extensional deformation. The differences observed were in the fourth or fifth significant figure as compared to the corresponding flap-lag-extensional equations' solution. For the geometric and physical parameters considered in this work, the extensional degree of freedom can thus be safely ignored. It is also observed that the mode shapes calculated about the deformed equilibrium position and obtained by using the present nonlinear equations do not differ to any appreciable extent from those obtained from the linear theory.

CONCLUDING REMARKS

Coupled flap-lag-extensional equations of motion of rotating, pretwisted cantilever blades of uniform rectangular cross section are derived including large precone, Coriolis effects and second degree geometric nonlinearities. Parametric studies are conducted to assess the individual and combined influence of the various complicating effects by solving the nonlinear equations using a linear pertubation technique. The following major conclusions have emerged from the present effort:

1. Inclusion of the geometric nonlinearities up through second degree only in the flap-lag-extension equations appears to be adequate for the prediction of steady-state deflections and the first few natural frequencies (if they are well separated from a basic torsional frequency) of thin blades having precones of up to 45°, and rotating at speeds of the order of $\Omega/\omega_1 = 1.0$.

The second degree geometric nonlinearities show a stiffining effect on the flatwise modes in general, and a softening effect on the first edgewise mode, for precones of up to 50° and for all rotational speeds considered in this work. The effect of geometric nonlinearities on higher modes is not significant. The greatest effect is from those nonlinear terms which vanish for zero precone. However, if precone is substantial, the second degree nonlinear terms can produce frequency changes of engineering significance. The increase in frequencies of first flatwise and first edgewise modes are typically of the respective orders of +20 percent and -4 percent for blades with 45° precone and for a rotational speed parameter of $\Omega/\omega_1 = 1.0$.

2. The effect of nonlinear Coriolis forces is most severe on the first flatwise and first edgewise modes, and insignificant on higher modes. The effect of Coriolis forces is found to be significant for thick blade cases. In general, the nonlinear Coriolis forces oppose the linear ones, the nonlinear effect being stronger. Thus, both linear and nonlinear Coriolis effects can be ignored in analyzing thin blades which are typical of advanced turboprop blade configurations.

3. Preconing has significant influence on the first flatwise and edgewise modes. An increase in precone at a given rotational speed shows a softening effect on flatwise modes generally, and a stiffening effect on the first edgewise mode. However, the softening effect is much more pronounced than the stiffening effect.

4. The coupling trends for pretwisted blades observed from the solution of the present nonlinear equations, do not differ to any appreciable extent from those observed from the linear theory. This may be attributed partially to the fact that geometric nonlinearities do not significantly affect higher modes for the present flap-lag-extensional equations.

APPENDIX A: THE GALERKIN INTEGRALS AND MODEL EQUATIONS

The various integrals arising from the Galerkin process are defined below, and these are used in representing the modal equations in matrix forms subsequently:

$$\delta_{ij} = \int_0^1 \psi_i \psi_j \, d\eta = \int_0^1 \theta_i \theta_j \, d\eta$$

$$A_{ijk} = \int_0^1 \psi_i \int_0^\eta \psi_j'(\bar{x}) \psi_k'(\bar{x}) \, d\bar{x} \, d\eta$$

$$B_{ij} = \int_0^1 \psi_i \psi_j'' Q \, d\eta$$

$$C_{ij} = \int_0^1 \psi_i \psi_j' S \, d\eta$$

$$D_{ijk} = \int_0^1 \psi_i \psi_j'' \int_\eta^1 \psi_k(\bar{x}) \, d\bar{x} \, d\eta$$

$$E_{ijk} = \int_0^1 \psi_i \psi_j'' \psi_k \, d\eta$$

$$F_{ij} = \int_0^1 \psi_i \psi_j^{iv} \left(\cos^2 \theta + \frac{b^2}{d^2} \sin^2 \theta \right) d\eta$$

$$G_{ij} = \int_0^1 \psi_i \psi_j''' \sin 2\theta \, d\eta$$

$$H_{ij} = \int_0^1 \psi_i \psi_j'' \cos 2\theta \, d\eta$$

$$I_{ij} = \int_0^1 \psi_i \psi_j^{iv} \sin 2\theta \, d\eta$$

$$J_{ij} = \int_0^1 \psi_i \psi_j''' \cos 2\theta \, d\eta$$

$$K_{ij} = \int_0^1 \psi_i \psi_j'' \sin 2\theta \, d\eta$$

$$L_i = \int_0^1 \psi_i \eta \, d\eta$$

$$M_{ij} = \int_0^1 \psi_i \psi_j^{iv} \left(\sin^2 \theta + \frac{b^2}{d^2} \cos^2 \theta \right) d\eta$$

$$N_{ij} = \int_0^1 \psi_i \psi_j'' \, d\eta$$

$$O_{ij} = \int_0^1 \psi_i \theta_j \, d\eta$$

$$P_{ijk} = \int_0^1 \theta_k \, d\eta \int_0^1 \psi_i \psi_j'' \, d\eta - \int_0^1 \psi_i \psi_j'' \int_0^\eta \theta_k(\bar{x}) \, d\bar{x} \, d\eta$$

$$Q_{ijk} = \int_0^1 \psi_i \psi_j' \theta_k \, d\eta$$

$$R_{ij} = \int_0^1 \theta_i \theta_j'' \, d\eta$$

$$S_i = \int_0^1 \theta_i \eta \, d\eta$$

$$T_{ijk} = \int_0^1 \theta_i \int_0^\eta \psi_j'(\bar{x}) \psi_k'(\bar{x}) \, d\bar{x} \, d\eta$$

$$u_i = \int_0^1 \psi_i \sin 2\theta \, d\eta$$

$$v_i = \int_0^1 \psi_i \cos 2\theta \, d\eta$$

The linear and nonlinear parts of the steady state equilibrium equations are presented below in the matrix form, $[\underset{\sim}{L} + \underset{\sim}{NL}]\{X_o\} = \{B\}$

$$
\left\{
\begin{array}{c|c|c}
\begin{array}{l}
\sin^2 \beta_{Pc}\delta_{ij} - \frac{1}{2}\sin\beta_{Pc}\cos\beta_{Pc}\sum_k w_{ok}A_{ijk} \\
- \cos^2\beta_{Pc}(B_{ij} - C_{ij}) + \sin\beta_{Pc}\cos\beta_{Pc} \times \\
\sum_k \left\{ v_{ok}D_{ijk} - w_{ok}E_{ijk} \right\} \\
+ \varepsilon\left[F_{ij} + 2\gamma\left(\frac{b^2}{d^2} - 1\right)G_{ij} + \right. \\
\left. 2\gamma^2\left(\frac{b^2}{d^2} - 1\right)H_{ij}\right]
\end{array}
&
\begin{array}{l}
-\frac{1}{2}\sin\beta_{Pc}\cos\beta_{Pc}\sum_k v_{ok}A_{ijk} + \\
\varepsilon\left(\frac{b^2}{d^2} - 1\right)\left\{\frac{1}{2}I_{ij} + 2\gamma J_{ij} - 2\gamma^2 K_{ij}\right\}
\end{array}
&
\begin{array}{l}
\sin\beta_{Pc}\cos\beta_{Pc}O_{ij} + \\
\cos^2\beta_{Pc}\sum_k w_{ok}(Q_{ikj} - P_{ikj})
\end{array}
\\ \hline
\begin{array}{l}
\cos\beta_{Pc}\sin\beta_{Pc}\sum_k (v_{ok}D_{ikj} - v_{ok}E_{ikj}) \\
+ \varepsilon\left(\frac{b^2}{d^2} - 1\right)\left\{\frac{1}{2}I_{ij} + 2\gamma J_{ij} - 2\gamma^2 K_{ij}\right\}
\end{array}
&
\begin{array}{l}
-\delta_{ij} - \cos^2\beta_{Pc}(B_{ij} - C_{ij}) + \\
\varepsilon\left\{M_{ij} - 2\gamma\left(\frac{b^2}{d^2} - 1\right)\left[G_{ij} - \right.\right. \\
\left.\left. - 2\gamma^2 \frac{b^2}{d^2} - 1)H_{ij}\right]\right\}
\end{array}
&
\cos^2\beta_{Pc}\sum_k v_{ok}(Q_{ikj} - P_{ikj})
\\ \hline
\begin{array}{l}
\frac{1}{2}\cos^2\beta_{Pc}\,{}_k\, w_{ok}T_{ijk} + \\
\sin\beta_{Pc}\cos\beta_{Pc}O_{ji}
\end{array}
&
\frac{1}{2}\cos^2\beta_{Pc}\sum_k v_{ok}T_{ijk}
&
\begin{array}{l}
-\cos^2\beta_{Pc}\delta_{ij} \\
-\frac{AE}{m\Omega^2 L^2}R_{ij}
\end{array}
\end{array}
\right\}
\left\{
\begin{array}{c}
w_{oj} \\ \hline v_{oj} \\ \hline u_{oj}
\end{array}
\right\}
=
\left\{
\begin{array}{l}
-\sin\beta_{Pc}\cos\beta_{Pc}L_i \\
-\left(\frac{\gamma I_{nn}}{AL^2}\right)\sin\beta_{Pc} \\
\times\cos\beta_{Pc}u_i\left(\frac{b^2}{d^2} - 1\right) \\ \hline
-\left(\frac{\gamma I_{nn}}{AL^2}\right)\sin\beta_{Pc} \\
\times\cos\beta_{Pc}v_i\left(\frac{b^2}{d^2} - 1\right) \\ \hline
\cos^2\beta_{Pc}S_i
\end{array}
\right\}
$$

The mass, Gyroscopic and stifness matrices resulting from the perturbation equations are designated $[\underset{\sim}{M}]$, $[\underset{\sim}{C}]$ and $[\underset{\sim}{K}]$ respectively, and are presented in the following:

$$[\underset{\sim}{M}] = \left[\begin{array}{c|c|c} \delta_{ij} & 0 & \sum_k w_{ok}(P_{ikj} - Q_{ikj}) \\ \hline 0 & \delta_{ij} & \sum_k v_{ok}(P_{ikj} - Q_{ikj}) \\ \hline -\sum_k w_{ok} T_{ijk} & -\sum_k v_{ok} T_{ijk} & \delta_{ij} \end{array}\right]$$

$$[\underset{\sim}{C}] = \left[\begin{array}{c|c|c} 0 & \begin{array}{c} 2 \sin \beta_{Pc}\, \delta_{ij} - \\ - 2 \cos \beta_{Pc} \sum_k w_{ok}(D_{ikj} - E_{ikj}) \end{array} & 0 \\ \hline \begin{array}{c} - 2 \sin \beta_{Pc}\, \delta_{ij} \\ - 2 \cos \beta_{Pc} \sum_k w_{ok} A_{ijk} \end{array} & \begin{array}{c} - 2 \cos \beta_{Pc} \sum_k v_{ok}(D_{ikj} - E_{ikj}) \\ - 2 \cos \beta_{Pc} \sum_k v_{ok} A_{ijk} \end{array} & 2 \cos \beta_{Pc}\, O_{ij} \\ \hline 0 & - 2 \cos \beta_{Pc}\, O_{ji} & 0 \end{array}\right]$$

$$
[\underset{\sim}{K}] = \left\{ \begin{array}{l|l|l}
\begin{array}{l}
- \sin^2 \beta_{Pc} \delta_{ij} - \cos^2 \beta_{Pc} (B_{ij} - C_{ij}) \\
- \sin \beta_{Pc} \cos \beta_{Pc} \sum_k w_{ok} A_{ijk} + \\
\sin \beta_{Pc} \cos \beta_{Pc} \sum_k w_{ok} \left[D_{ijk} + D_{ikj} - E_{ijk} - E_{ikj} \right] \\
+ \epsilon \left[F_{ij} + 2\gamma \left(\frac{b^2}{d^2} - 1 \right) (G_{ij} + \gamma H_{ij}) \right] \\
+ \cos^2 \beta_{Pc} \sum_k u_{ok} (Q_{ijk} - P_{ijk})
\end{array}
&
\begin{array}{l}
- \sin \beta_{Pc} \cos \beta_{Pc} \sum_k v_{ok} A_{ijk} \\
+ \epsilon \left[\frac{1}{2} I_{ij} + 2\gamma (J_{ij} - \gamma K_{ij}) \right] \left(\frac{b^2}{d^2} - 1 \right)
\end{array}
&
\begin{array}{l}
\sin \beta_{Pc} \cos \beta_{Pc} O_{ij} \\
+ \cos^2 \beta_{Pc} \sum_k w_{ok} (Q_{ikj} - P_{ikj})
\end{array}
\\ \hline
\begin{array}{l}
\sin \beta_{Pc} \cos \beta_{Pc} \sum_k v_{ok} (D_{ikj} - E_{ikj}) \\
+ \epsilon \left[\frac{1}{2} I_{ij} + 2\gamma J_{ij} - 2\gamma^2 K_{ij} \right] \left(\frac{b^2}{d^2} - 1 \right)
\end{array}
&
\begin{array}{l}
- \delta_{ij} - \cos \beta_{Pc} (B_{ij} - C_{ij}) \\
+ \sin \beta_{Pc} \cos \beta_{Pc} \sum_k w_{ok} (D_{ijk} - E_{ijk}) \\
+ \epsilon \left[M_{ij} - 2\gamma \left(\frac{b^2}{d^2} - 1 \right) (G_{ij} + \gamma H_{ij}) \right] \\
+ \cos^2 \beta_{Pc} \sum_k u_{ok} (Q_{ijk} - P_{ijk})
\end{array}
&
\begin{array}{l}
\cos^2 \beta_{Pc} \sum_k v_{ok} (Q_{ikj} - P_{ikj})
\end{array}
\\ \hline
\begin{array}{l}
\sin \beta_{Pc} \cos \beta_{Pc} O_{ji} \\
+ \cos^2 \beta_{Pc} \sum_k w_{ok} T_{ijk}
\end{array}
&
\begin{array}{l}
\cos^2 \beta_{Pc} \sum_k v_{ok} T_{ijk}
\end{array}
&
\begin{array}{l}
- \cos^2 \beta_{Pc} \delta_{ij} \\
- \frac{AE}{m\Omega^2 L^2} R_{ij}
\end{array}
\end{array} \right\}
$$

APPENDIX B - NOMENCLATURE

A	cross-sectional area of blade
A_{ijk}, B_{ij}, L_i, etc.	modal integrals (see appendix A)
b, d	breadth (chord) and thickness of blade
d/b	thickness ratio
$\{B\}$, $\{X\}$, $\{X_0\}$	vectors
$[\underset{\sim}{C}]$	modal damping matrix (gyroscopic matrix)
E	Young's modulus
$I_{\eta\eta}$, $I_{\xi\xi}$	area moments of inertia about major and minor principal centroidal axes, respectively
i, j, k	dummy indices
L	length of beam
$[\underset{\sim}{L}]$, $[\underset{\sim}{LN}]$	Linear and nonlinear components of the matrix representing steady state equilibrium equations
m	mass of blade per unit length
$[\underset{\sim}{M}]$	modal mass matrix
n	number of nonrotating modes for each of the flap bending, lead-lag bending, and extensional deflections
p	natural radian frequency
R	radius of disc
T	blade tension
t	time
u, v, w	displacements of the elastic axis in X, Y, Z directions, respectively
$\bar{u}$, $\bar{v}$, $\bar{w}$	dimensionaless deflections
u_{oj}, v_{oj}, w_{oj}	steady-state equilibrium deflections
Δu_j, Δv_j, Δw_j	perturbation quantities

x	running coordinate along X-axis
y, z	centroidal principal axes of beam cross section
α_j, β_j, γ_j	constants for assumed mode shapes
β_{Pc}	precone angle
γ	total pretwist of the blade over its length
δ_{ij}	Kronecker delta
ξ	nondimensional rotational parameter, $EI_{\eta\eta}/\rho AL^4\Omega^2$
η	nondimensional length coordinate, x/L
θ	geometric pitch angle, $\varphi + \gamma\eta$
λ_1	frequency parameter, $\sqrt{EI_{\eta\eta}/\rho AL^4}$
ρ	mass density of blade material
φ	setting angle (collective pitch)
$\Psi_j(\eta)$	nonrotating flap and lead-lag bending mode shapes
τ	dimensionless time, Ωt
ω_1	exact fundamental mode frequency of straight, nonrotating beam, $3.51602 \ \lambda_1$
Ω	rotor blade angular velocity, rad/sec
$(\ )'$	primes denote differentiation with respect to x or η
$(\dot{\ })$	dot over a parameter represents differentiation with respect to t or τ

REFERENCES

1. Rao, J.S.: Turbomachine Blade Vibration. Shock and Vibration Digest, vol. 15, no. 5, May 1983, pp. 3-9.

2. Leissa, A.: Vibrational Aspects of Rotating Turbomachinery Blades. Appl. Mech. Rev., vol. 34, no. 5, May 1981, pp. 629-635.

3. Friedmann, Peretz P.: Recent Developments in Rotary - Wing Aeroelasticity. J. Aircr., vol. 14, no. 11, Nov. 1977, pp. 1027-1041.

4. Houbolt, John C.; and Brooks, George W.: Differential Equations of Motion for Combined Flapwise Bending, Chordwise Bending, and Torsion of Twisted Nonuniform Rotor Blades. NACA Report 1346, 1958.

5. Carnegie, W.: A Note on the Application of the Variational Method to Derive the Equations of Dynamic Motion of a Pretwisted Cantilever Blade Mounted on the Periphery of a Rotating Disc Allowing for Shear Deflection, Rotary Inertia and Torsion Bending. Bulletin Mechanical Engineering Education, vol. 5, 1966, pp. 221-223.

6. Subrahmanyam, K.B.; Kulkarni, S.V.; and Rao, J.S.: Application of the Reissner Method to Derive the Coupled Bending-Torsion Equations of Dynamic Motion of Rotating Pretwisted Cantilever Blading with Allowance for Shear Deflection, Rotary Inertia, Warping and Thermal Effects. J. Sound Vibr., vol. 84, no. 2, Sept. 22, 1982, pp. 223-240.

7. Hodges, D.H.; and Dowell, E.H.: Nonlinear Equations of Motion for the Elastic Bending and Torsion of Twisted Nonuniform Rotor Blades. NASA TN-D-7817, 1974.

8. Rosen, A.; and Friedmann, P.P.: Nonlinear Equations for Elastic Helicopter or Wind Turbine Blades Undergoing Moderate Deformation. University of California, Los Angeles, School of Engineering and Applied Science Report, UCLA-ENG-7718, Dec. 1978.

9. Kaza, K.R.V.; and Kvaternik, R.G.: Nonlinear Aeroelastic Equations for Combined Flapwise Bending, Chordwise Bending, Torsion and Extension of Twisted Non-Uniform Rotor Blades in Forward Flight. NASA TM-74059, 1977.

10. Subrahmanyam, K.B.; and Kaza, K.R.V.: Vibration and Buckling of Rotating, Pretwisted, Preconed Beams Including Coriolis Effects. NASA TM-87004, 1985. (To be presented at the 10th Biennial ASME Design Engineering Conference and Exhibit on Mechanical Vibration and Noise, Cincinnati, OH, Sept. 10-13, 1985.)

11. Kvaternik, R.G.; White, W.F.; and Kaza, K.R.V.: Nonlinear Flap-Lag-Axial Equations of a Rotating Beam with Arbitrary Precone Angle. AIAA Paper 78-491, 1978.

12. Chang, Tish-Chun.; and Craig, R.R., Jr.: On Normal Modes of Uniform Beams. Engineering Mechanics Research Laboratory, University of Texas, EMRL 1068, 1969.

13. The International Mathematical and Statistical Library (IMSL). Houston, TX, Edition 9, Revision, June 1, 1982.

14. Leissa, A.; and Co, C.: Coriolis Effects on the Vibration of Rotating Beams and Plates. Proceedings of XII SECTAM Conference, Callaway Gardens, Vol. II, Auburn University, AL, 1984, pp. 508-513.

TABLE I. - CONVERGENCE PATTERN OF FREQUENCY RATIOS (p/λ_1) OF A PRECONED, ROTATING BEAM PRODUCED BY THE GALERKIN METHOD WITH NONROTATING NORMAL MODES

[$\Omega/\omega 1 = 0.5$, $\beta_{PC} = 30^\circ$, $d/b = 0.5$, $L/d = 20$, $\varphi = 0^\circ$, $\gamma = R = 0$.]

(a) Frequencies from solution of linear equations ignoring Coriolis effects

Mode	n = 1	n = 2	n = 3	n = 4	n = 5
1	3.788724	3.788037	3.787921	3.787906	3.787903
2	7.008871	7.008777	7.008761	7.008758	7.008758
3	108.883020	22.355387	22.355386	22.355314	22.355303
4	----------	44.204056	44.204056	44.204047	44.204045
5	----------	108.882980	62.025490	62.025447	62.025401

(b) Frequencies from solution of linear equations including Coriolis effects

Mode	n = 1	n = 2	n = 3	n = 4	n = 5
1	3.635308	3.634662	3.634553	3.634539	3.634535
2	7.302023	7.301872	7.301851	7.301849	7.301848
3	108.92232	22.331668	22.331666	22.331595	22.331584
4	----------	44.247993	44.247881	44.247870	44.247867
5	----------	108.92610	62.017091	62.017048	62.017003

(c) Frequencies from perturbation solution of nonlinear equations: Coriolis effects ignored

Mode	n = 1	n = 2	n = 3	n = 4	n = 5
1	3.847417	3.846369	3.846218	3.846199	3.846194
2	7.019543	7.019438	7.019422	7.019420	7.019419
3	109.47317	22.378138	22.378096	22.378012	22.377999
4	----------	44.213271	44.213273	44.213263	44.213262
5	----------	109.57995	61.959160	61.958438	61.958267

(d) Frequencies from perturbation solution of nonlinear equations: Coriolis effects included

Mode	n = 1	n = 2	n = 3	n = 4	n = 5
1	3.742021	3.740674	3.740498	3.740475	3.740470
2	7.214380	7.214485	7.214484	7.214484	7.214484
3	109.51676	22.363212	22.363188	22.363103	22.363090
4	----------	44.242350	44.241858	44.241828	44.241822
5	----------	109.62655	61.954879	61.954157	61.953988

TABLE II. - COMPARISON OF FREQUENCY PARAMETER RATIOS, ($f = p/\lambda_1$), OF ROTATING BLADES FROM BEAM THEORY AND MSC NASTRAN

[$\beta_{PC} = \varphi = \gamma = 0^\circ$, $(d/b) = 0.05$.]

$\frac{\Omega}{\omega_1}$	Mode (a)	MSC NASTRAN	Beam theory (non-linear)	Percent frequency difference[b]	$\frac{\Omega}{\omega_1}$	Mode (a)	MSC NASTRAN	Beam theory (non-linear)	Percent frequency difference[b]
0.5	F1	3.5463	3.5213	0.705	1.00	F1	5.2142	5.1917	0.432
	F2	22.1496	22.0390	0.499		F2	23.8828	23.7831	0.418
	F3	61.9732	61.7017	0.438		F3	63.7103	63.4591	0.394
	T1	68.3947	---------	------		T1	68.5803	---------	------
	S1	69.9391	70.3203	-0.545		S1	69.9556	70.3359	-0.544
	F4	121.4804	120.9065	0.472		F4	123.2737	122.7303	0.441
	F5	201.0141	199.8640	0.572		F5	202.8394	201.7327	0.546
	T2	206.2487	---------	------		T2	206.5022	---------	------
0.50	F1	4.0287	4.0049	0.591	1.20	F1	5.7917	5.7694	0.385
	F2	22.5920	22.4843	0.477		F2	24.6085	24.5132	0.387
	F3	62.4092	62.1428	0.427		F3	64.4601	64.2176	0.376
	T1	68.4408	---------	------		T1	68.6620	---------	------
	S1	69.9432	70.3242	-0.545		S1	69.9629	70.3428	-0.543
	F4	121.9282	121.3618	0.465		F4	124.0553	123.5262	0.427
	F5	201.4689	200.3292	0.566		F5	203.6387	202.5524	0.534
	T2	206.3116	---------	------		T2	206.6139	---------	------
0.80	F1	4.6850	4.6621	0.489	1.50	F1	6.7182	6.6958	0.333
	F2	23.2721	23.1687	0.444		F2	25.8909	25.8031	0.339
	F3	63.0895	62.8310	0.410		F3	65.8156	65.5890	0.344
	T1	68.5134	---------	------		T1	68.8120	---------	------
	S1	69.9497	70.3303	-0.544		S1	69.9763	70.3555	-0.542
	F4	122.6299	122.0756	0.452		F4	125.4796	124.9769	0.401
	F5	202.1829	201.0600	0.555		F5	205.1007	204.0542	0.510
	T2	206.4108	---------	------		T2	206.8193	---------	------

[a]F1, F2,.. F5 are frequencies in flatwise direction; S1 is first edgewise frequency and T1 and T2 are the lowest two torsional mode frequencies respectively.
[b]Percent frequency difference = ($f_{NASTRAN} - f_{Nonlinear}$)x100/$f_{NASTRAN}$.

TABLE III. - COMPARISON OF LINEAR AND PERTURBATION FREQUENCIES OF PRECONED BLADE AT VARIOUS ROTATIONAL SPEEDS

[B_{pc} = 15°, ϕ = R = 0, Thickness ratio = 0.05.]

$\frac{\Omega}{\omega_1}$	Mode	Beam Theary Results (Coriolis Effects Included)			MSC NASTRAN Coriolis effects neglected	$\left[\frac{f_{Nastran} - f_{Nonlinear}}{f_{Nastran}}\right]$x100
		Linear	Nonlinear	Percent frequency change[a]		
0.3	1	3.6776	3.6804	0.076	3.7062	0.696
	2	22.1849	22.1860	0.005	22.2934	0.482
	3	61.8467	61.8475	0.001	62.1044	0.414
0.5	1	3.9476	3.9652	0.444	3.9950	0.746
	2	22.4498	22.4572	0.033	22.5585	0.449
	3	62.1113	62.1169	0.009	62.3354	0.351
0.8	1	4.5356	4.6094	1.601	4.6451	0.769
	2	23.0828	23.1182	0.153	23.2026	0.364
	3	62.7514	62.7763	0.397	62.8837	0.171
1.0	1	5.0138	5.1444	2.539	5.1781	0.651
	2	23.6522	23.7203	0.287	23.7926	0.304
	3	63.3360	63.3821	0.073	63.4078	0.041
2.0	1	7.8855	8.3777	5.875	8.3385	-0.470
	2	27.9477	28.3037	0.444	28.3445	0.144
	3	67.9947	68.0724	0.114	68.0883	0.023

[a]Percent frequency change = ($f_{nonlinear}$ - f_{linear})x100/$f_{nonlinear}$.

TABLE IV. - FURTHER COMPARISON OF FREQUENCY PARAMETER RATIOS, ($f = p/\lambda_1$), FROM MSC NASTRAN AND FROM BEAM THEORY FOR VARIOUS PRECONES, ROTATIONAL SPEEDS AND THICKNESS RATIOS

d/b	B_{pc} deg	$\frac{\Omega}{\omega_1}$	Mode	MSC NASTRAN	Beam theory	Percent frequency difference[a]	d/b	B_{pc} deg	$\frac{\Omega}{\omega_1}$	Mode	MSC NASTRAN	Beam theory	Percent frequency difference[a]
0.05	30	0.9	1	4.7719	4.6937	1.639	0.05	45	0.445	1	3.6511	3.6066	1.219
			2	23.2410	23.2313	0.042				2	22.2438	22.2087	0.158
			3	62.4392	62.8783	-0.703				3	61.8224	61.8820	-0.096
0.05	45	0.8	1	4.2769	4.1026	4.075	0.05	45	1.0	1	4.8337	4.6145	4.535
			2	22.6971	22.7218	-0.109				2	23.1064	23.2047	-0.425
			3	61.6110	62.3800	-1.248				3	61.4499	62.8250	-2.238
0.05	45	1.05	1	4.9615	4.7622	4.017	0.05	60	0.5	1	3.4708	3.3944	2.201
			2	23.2508	23.3468	-0.413				2	22.2377	22.1264	0.501
			3	61.6563	62.9538	-2.104				3	62.0111	61.8150	0.316
0.25	45	0.8	1	4.2598	4.0236 [b]4.1058	5.545 [b]3.615	0.25	45	1.0	1	4.8122	4.5128 [b]4.6185	6.222 [b]4.025
			2	12.8590	14.2623 [b]13.9954	-10.913 [b]-8.837				2	12.3085	14.2650 [b]13.9808	-15.896 [b]-13.587
			3	22.6460	22.7315 [b]22.7209	-0.378 [b]-0.331				3	23.0257	23.2460 [b]23.2040	-0.957 [b]-0.774

[a]Percent frequency difference = ($f_{NASTRAN}$ - $f_{nonlinear}$)x100/$f_{NASTRAN}$.

[b](Coriolis effects are included in beam theory in all cases except where marked and are absent in MSC NASTRAN calculations) $\phi = \gamma = 0°$, R = 0.

ORIGINAL PAGE IS OF POOR QUALITY

TABLE V. - COMPARISON OF LINEAR AND PURTURBATION FREQUENCIES OF ROTATING BLADES AT VARIOUS PRECONE ANGLES (CORIOLIS EFFECTS INCLUDED): $\Omega/\omega_1 = 1.0$, $\varphi = 0^\circ$, $\bar{\delta} = 0$

β_{pc}	Mode	Low thickness ratio, d/b = 0.05			High thickness ratio, d/b = 0.25		
		Linear	Nonlinear	Percent frequency variation[a]	Linear	Nonlinear	Percent frequency variation[a]
10	1	5.1124	5.1713	1.139	5.0912	5.1680	1.486
	2	23.7242	23.7553	0.131	14.1663	14.1229	-0.307
	3	63.4037	63.4246	0.033	23.7219	23.7606	0.163
20	1	4.8770	5.1043	4.453	4.8009	5.0865	5.615
	2	23.5540	23.6709	0.494	14.2935	1[illegible] 1313	-1.148
	3	63.2440	63.3234	0.125	23.5450	23.6854	0.[illegible]93
30	1	4.4930	4.9749	9.687	4.3492	4.9316	11.810
	2	23.2908	23.5282	1.009	14.477[illegible]	14.1553	-2.273
	3	62.9985	63.1612	0.258	23.2718	23.5526	1.192
40	1	3.9725	4.7610	16.562	3.7715	4.6814	19.437
	2	22.9639	23.5266	1.555	14.6859	14.2072	-3.369
	3	62.6960	62.9476	0.400	22.9329	23.3554	1.809
45	1	3.6659	4.6145	20.557	3.4464	4.5133	23.639
	2	22.7880	23.2047	1.796	14.7907	14.2477	-3.811
	3	62.5344	62.8250	0.463	22.7509	23.2316	2.069
50	1	3.3315	4.4371	24.917	3.1023	4.3129	28.069
	2	22.6109	23.0697	1.989	14.8916	14.3002	-4.136
	3	62.3724	62.6942	0.513	22.5677	23.0910	2.266

[a]Percent frequency variation = $(\omega_{nonlinear} - \omega_{linear}) \times 100/\omega_{nonlinear}$.

TABLE VI. - EFFECT OF LINEAR AND NONLINEAR CORIOLIS FORCES, AND VARIOUS NONLINEAR TERMS ON THE FREQUENCY PARAMETER RATIOS FOR UNTWISTED THIN BLADES

(a) $d/b = 0.05$, $\phi = 0^\circ$, $\gamma = 0^\circ$, $\bar{R} = 0$

β_{pc}	$\frac{\Omega}{\omega_1}$	Mode	Solution of linear equations		Perturbation solution of nonlinear equations					
			Coriolis forces included	Coriolis forces ignored	Full nonlinear equation	Linear Coriolis forces ignored	Nonlinear Coriolis forces ignored	$A_{ijk} = 0$[a]	$D_{ijk} = 0$[b] $E_{ijk} = 0$[b]	$D_{ijk} = 0$ $E_{ijk} = 0$ $P_{ijk} = 0$[c] $Q_{ijk} = 0$[c]
15°	0.5	1	3.9476	3.9480	3.9652	3.9654	3.9650	3.9593	3.9535	3.9535
		2	22.4498	22.4498	22.4572	22.4572	22.4572	22.4563	22.4507	22.4507
		3	62.1113	62.1114	62.1169	62.1169	62.1173	62.1170	62.1115	62.1117
	0.8	1	4.5356	4.5366	4.6094	4.6096	4.6087	4.5852	4.5608	4.5608
		2	23.0828	23.0829	23.1182	23.1182	23.1185	23.1142	23.0873	23.0874
		3	62.7514	62.7515	62.7763	62.7763	62.7807	62.7792	62.7525	62.7531
	1.0	1	5.0138	5.0155	5.1444	5.1443	5.1431	5.1021	5.0589	5.0589
		2	23.6522	23.6524	23.7203	23.7202	23.7210	23.7131	23.6611	23.6611
		3	63.3360	63.3361	63.3821	63.3820	63.3936	63.3909	63.3383	63.3394
45°	0.5	1	3.5553	3.5576	3.6482	3.6 98	3.6476	3.6180	3.5872	3.5872
		2	22.2252	22.2256	22.2616	22.2618	22.2616	22.2574	22.2299	22.2299
		3	61.9077	61.9078	61.9351	61.9352	61.9364	61.9350	61.9083	61.9094
	0.8	1	3.6141	3.6199	4.1026	4.1050	4.0991	3.9591	3.7994	3.7994
		2	22.5196	22.5206	22.7218	22.7221	22.7230	22.7050	22.5476	22.5478
		3	62.2344	62.2348	62.3800	62.3800	62.3976	62.3943	62.2388	62.2448
	1.0	1	3.6659	3.6751	4.6145	4.6164	4.6069	4.3631	4.0621	4.0621
		2	22.7880	22.7895	23.2047	23.2045	23.2080	23.1816	22.8500	22.8504
		3	62.5344	62.5349	62.8250	62.8246	62.8761	62.8784	62.5451	62.5576
90°	0.5	1	3.0412	3.0450	3.0412	3.0450	3.0412	3.0412	3.0412	3.0412
		2	21.9636	21.9643	21.9636	21.9643	21.9636	21.9636	21.9636	21.9636
		3	61.6719	61.6722	61.6719	61.6722	61.6719	61.6719	61.6719	61.6719
	0.8	1	2.1029	2.1096	2.1029	2.1096	2.1029	2.1029	2.1029	2.1029
		2	21.8524	21.8542	21.8524	21.8542	21.8524	21.8524	21.8524	21.8524
		3	61.6324	61.6331	61.6324	61.6331	61.6324	61.6324	61.6324	61.6321
	1.0	1	unstable	unstable	unstable	unstable	unstable	unstable	unstable	unstable
		2	--------	--------	--------	--------	--------	--------	--------	--------
		3	--------	--------	--------	--------	--------	--------	--------	--------

[a]Nonlinear terms due to foreshortening are ignored.
[b]Nonlinear terms arising from $(Tv')'$ and $(Tw')'$ are ignored.
[c]Nonlinear terms associated with extentional deformation are ignored.

TABLE VI. - EFFECT OF LINEAR AND NONLINEAR CORIOLIS FORCES, AND VARIOUS NONLINEAR COUPLING TERMS ON THE FREQUENCY PARAMETER RATIOS FOR PRETWISTED THIN BLADES

(b) $d/b = 0.05$, $\phi = 0^\circ$, $\gamma = 30^\circ$, $R = 0$

β_{pc}	$\frac{\Omega}{\omega_1}$	Mode	Solution of linear equations		Perturbation solution of nonlinear equations					
			Coriolis forces included	Coriolis forces ignored	Full nonlinear equation	Linear Coriolis forces ignored	Nonlinear Coriolis forces ignored	$A_{ijk} = 0$	$D_{ijk} = 0$ $E_{ijk} = 0$	$D_{ijk} = 0$ $E_{ijk} = 0$ $P_{ijk} = 0$ $Q_{ijk} = 0$
15°	0.5	1	3.9540	3.9551	3.9716	3.9772	3.9711	3.9657	3.9600	3.9599
		2	20.0667	20.0621	20.0716	20.0688	20.0733	20.0715	20.0664	20.0664
		3	59.0449	59.0442	59.0499	59.0497	59.0504	59.0499	59.0449	59.0450
	0.8	1	4.5355	4.5388	4.6099	4.6107	4.6079	4.5855	4.5613	4.5613
		2	20.6248	20.6132	20.6488	20.6460	20.6563	20.6477	20.6232	20.6232
		3	59.6203	59.6184	59.6442	59.6447	59.6470	59.6441	59.6199	59.6202
	1.0	1	5.0092	5.0147	5.1416	5.1417	5.1374	5.0986	5.0557	5.0557
		2	21.1262	21.1082	21.1731	21.1724	21.1869	21.1700	21.1225	21.1225
		3	60.1438	60.1408	60.1903	60.1922	60.1962	60.1904	60.1428	60.1434
45°	0.5	1	3.55[illegible]	3.5672	3.6519	3.6578	3.6499	3.6216	3.5913	3.5913
		2	19.8932	19.[illegible]	19.9169	19.8912	19.9252	19.9171	19.8922	19.8922
		3	58.8651	[illegible].8594	58.8890	58.8857	58.8915	58.8889	58.8647	58.8653
	0.8	1	3.6066	3.6265	4.0952	4.1046	4.0841	3.9503	3.7928	3.7928
		2	20.1907	20.1035	20.3266	20.2884	20.3700	20.3268	20.1820	20.1821
		3	59.1652	59.1505	59.2997	59.2983	59.3148	59.3035	59.1620	59.1654
	1.0	1	3.6481	3.6791	4.6005	4.6089	4.5765	4.3454	4.0477	4.0477
		2	20.4614	20.3265	20.7467	20.7138	20.8328	20.7483	20.4387	20.4388
		3	59.4402	59.4172	59.7200	59.7250	59.7531	59.7361	59.4320	59.4388

TABLE VII. - EFFECT OF LINEAR AND NONLINEAR CORIOLIS FORCES, AND VARIOUS NONLINEAR COUPLING TERMS ON THE FREQUENCY PARAMETER RATIOS FOR THICK BLADES

(a) $d/b = 0.25, \varphi = 0^\circ, \gamma = 0^\circ, \bar{R} = 0$

β_{pc}	$\frac{\Omega}{\omega_1}$	Mode	Solution of linear equations		Perturbation solution of nonlinear equations					
			Coriolis forces included	Coriolis forces ignored	Full nonlinear equation	Linear Coriolis forces ignored	Nonlinear Coriolis forces ignored	$A_{ijk} = 0$	$D_{ijk} = 0$ $E_{ijk} = 0$	$D_{ijk} = 0$ $E_{ijk} = 0$ $P_{ijk} = 0$ $Q_{ijk} = 0$
15°	0.5	1	3.9390	3.9480	3.9600	3.9650	3.9565	3.9527	3.9469	3.9468
		2	14.1019	14.0765	14.0905	14.0793	14.1034	14.0964	14.0947	14.0948
		3	22.4485	22.4498	22.4568	22.4575	22.4556	22.4550	22.4494	22.4497
	0.8	1	4.5097	4.5365	4.6011	4.6055	4.5831	4.5707	4.5464	4.5458
		2	14.1628	14.0958	14.1117	14.1154	14.1702	14.1351	14.1268	14.1270
		3	23.0795	23.0829	23.1215	23.1223	23.1142	23.1111	23.0842	23.0852
	1.0	1	4.9684	5.0154	5.1351	5.1324	5.0977	5.0816	5.0388	5.0376
		2	14.2210	14.1134	14.1258	14.1598	14.2358	14.1654	14.1486	14.1488
		3	23.6470	23.6524	23.7297	23.7302	23.7146	23.7090	23.6570	23.6579
45°	0.5	1	3.4993	3.5575	3.6057	3.6486	3.5900	3.5690	3.5387	3.5387
		2	14.2495	14.0196	14.1940	14.0310	14.2570	14.2234	14.2150	14.2155
		3	22.2162	22.2256	22.2544	22.2614	22.2499	22.2469	22.2194	22.2220
	0.8	1	3.4722	3.6198	4.0238	4.0880	3.9369	3.8522	3.6990	3.6989
		2	14.5337	13.9500	14.2520	14.0405	14.5808	14.3878	14.3300	14.3331
		3	22.4961	22.5206	22.7230	22.7332	22.6865	22.6747	22.5167	22.5308
	1.0	1	3.4464	3.6747	4.5133	4.5621	4.3263	4.2119	3.9309	3.9308
		2	14.7907	13.8854	14.2478	14.1138	14.8973	14.4868	14.3435	14.3499
		3	22.7509	22.7895	23.2316	23.2414	23.1473	23.1333	22.7998	22.8273

TABLE VII. - EFFECT OF LINEAR AND NONLINEAR CORIOLIS FORCES, AND VARIOUS NONLINEAR COUPLING TERMS ON THE FREQUENCY PARAMETER RATIOS FOR PRETWISTED THICK BLADES

(b) $d/b = 0.25, \varphi = 0^\circ, \bar{R} = 0\ \gamma_t = 30^\circ$

β_{pc}	$\frac{\Omega}{\omega_1}$	Mode	Solution of linear equations		Perturbation solution of nonlinear equations					
			Coriolis forces included	Coriolis forces ignored	Full nonlinear equation	Linear Coriolis forces ignored	Nonlinear Coriolis forces ignored	$A_{ijk} = 0$	$D_{ijk} = 0$ $E_{ijk} = 0$	$D_{ijk} = 0$ $E_{ijk} = 0$ $P_{ijk} = 0$ $Q_{ijk} = 0$
15°	0.5	1	3.9439	3.9538	3.9649	3.9705	3.9611	3.9576	3.9518	3.9517
		2	13.2169	13.1901	13.2064	13.1937	13.2191	13.2120	13.2098	13.2099
		3	24.0327	24.0341	24.0394	24.0408	24.0388	24.0381	24.0331	24.0335
	0.8	1	4.5074	4.5369	4.5995	4.6048	4.5800	4.5687	4.5446	4.5441
		2	13.3419	13.2712	13.2948	13.2944	13.3524	13.3169	13.3061	13.3062
		3	24.5895	24.5933	24.6244	24.6279	24.6198	24.6164	24.5923	24.5936
	1.0	1	4.9606	5.0122	5.1294	5.1273	5.0888	5.0750	5.0325	5.0313
		2	13.4530	13.3393	13.3642	13.3926	13.4734	13.4016	13.3805	13.3804
		3	25.0954	25.1018	25.1659	25.1711	25.1554	25.1492	25.1022	25.1037
45°	0.5	1	3.5016	3.5658	3.6075	3.6553	3.5907	3.5708	3.5410	3.5410
		2	13.3418	13.1097	13.2916	13.1247	13.3530	13.3197	13.3084	13.3089
		3	23.8329	23.8359	23.8630	23.8664	23.8616	23.8578	23.8337	23.8367
	0.8	1	3.4631	3.6246	4.0136	4.0863	3.9205	3.8410	3.6897	3.6896
		2	13.6592	13.0703	13.4067	13.1819	13.7269	13.5344	13.4611	13.4639
		3	24.0827	24.0918	24.2659	24.2760	24.2461	24.2301	24.0899	24.1062
	1.0	1	3.4281	3.6766	4.4952	4.5530	4.2956	4.1909	3.9127	3.9126
		2	13.9447	13.0318	13.4582	13.3039	14.0933	13.6823	13.5075	13.5130
		3	24.3105	24.3268	24.7071	24.7230	24.6541	24.6313	24.3319	24.3640

TABLE VIII. - EFFECT OF LINEAR AND NONLINEAR CORIOLIS FORCES, AND VARIOUS NONLINEAR TERMS ON THE FREQUENCY PARAMETER RATIOS

[Presented as percent frequency variation based upon full nonlinear equation solution, $(f_{nonlinear} - f_{reference})\times 100/f_{nonlinear}$.]

(a) $\beta_{PC} = 15^\circ$, $\phi = \gamma = 0^\circ$, R = 0

$\frac{\Omega}{\omega_1}$	Mode	All nonlinear terms ignored	Linear Coriolis forces ignored	Nonlinear Coriolis forces ignored	$A_{ijk} = 0$	$D_{ijk} = 0$, $E_{ijk} = 0$
Thin blade: (d/b) = 0.05						
0.5	1	0.4439	-0.0050	0.0050	0.1488	0.2951
0.8	1	1.6011	-0.0043	0.0152	0.5250	1.0544
1.0	1	2.5387	0.0019	0.0253	0.8223	1.6620
0.5	2	0.0330	0.0	0.0	0.0040	0.0289
0.8	2	0.1531	0.0	-0.0013	0.0173	0.1337
1.0	2	0.2871	0.0004	-0.0030	0.0304	0.2496
0.5	3	0.0090	0.0	-0.0036	-0.0001	0.0087
0.8	3	0.0397	0.0	-0.0070	-0.0046	0.0379
1.0	3	0.0727	0.0002	-0.0181	-0.0139	0.0691
Thick blade: (d/b) = 0.25						
0.5	1	0.5303	-0.1263	0.0884	0.1843	0.3308
0.8	1	1.9865	-0.0956	0.3912	0.6607	1.1889
1.0	1	3.2463	0.0526	0.7283	1.0419	1.8753
0.5	2	-0.0809	0.0795	-0.0916	-0.0419	-0.0298
0.8	2	-0.3621	-0.0262	-0.4146	-0.1658	-0.1070
1.0	2	-0.6739	-0.2407	-0.7787	-0.2803	-0.1614
0.5	3	0.0370	-0.0031	0.0053	0.0080	0.0330
0.8	3	0.1817	-0.0035	0.0316	0.0450	0.1613
1.0	3	0.3485	-0.0021	0.0636	0.0872	0.3064

(b) $\beta_{PC} = 45^\circ$, $\phi = \gamma = 0^\circ$, R = 0.]

$\frac{\Omega}{\omega_1}$	Mode	All nonlinear terms ignored	Linear Coriolis forces ignored	Nonlinear Coriolis forces ignored	$A_{ijk} = 0$	$D_{ijk} = 0$, $E_{ijk} = 0$
Thin blade: (d/b) = 0.05						
0.5	1	2.5465	-0.0439	0.0165	0.8278	1.9188
0.8	1	11.9071	-0.0550	0.0853	3.4978	7.3904
1.0	1	20.5569	-0.0412	0.1647	5.4480	11.9710
0.5	2	0.1635	-0.0009	0.0	0.0189	0.1424
0.8	2	0.8899	-0.0001	-0.0053	0.0739	0.7667
1.0	2	1.7958	0.0009	-0.0142	0.0996	1.5286
0.5	3	0.0442	-0.0002	-0.0021	0.0002	0.0433
0.8	3	0.2334	0.0	-0.0282	-0.0229	0.2264
1.0	3	0.4626	0.0006	-0.0813	-0.0850	0.4455
Thick blade: (d/b) = 0.25						
0.5	1	2.9509	-1.1898	0.4354	1.1078	1.8582
0.8	1	13.7084	-1.5955	2.1597	4.2646	8.0720
1.0	1	23.6390	-1.0813	4.1433	6.6780	12.9041
0.5	2	-0.3910	1.1484	-0.4439	-0.2071	-0.1480
0.8	2	-1.9766	1.4840	-2.3071	-0.9529	-0.5471
1.0	2	-3.8104	0.9405	-4.5586	-1.6775	-0.6717
0.5	3	0.1717	-0.0315	0.0202	0.0337	0.1573
0.8	3	0.9986	-0.0449	0.1606	0.2126	0.9079
1.0	3	2.0692	-0.0422	0.3629	0.4231	1.8587

TABLE IX. - EFFECT OF LINEAR AND NONLINEAR CORIOLIS FORCES, AND VARIOUS NONLINEAR TERMS ON THE FREQUENCY PARAMETER RATIOS

[Presented as percent frequency variation based upon full nonlinear equation solution.]

(a) $\beta_{pc} = 15°$, $\varphi = 0°$, $R = 0$, $\gamma = 30°$

$\frac{\Omega}{\omega_1}$	Mode	All nonlinear terms ignored	Linear Coriolis forces ignored	Nonlinear Coriolis forces ignored	$A_{ijk} = 0$	$D_{ijk} = 0$, $E_{ijk} = 0$
Thin blade: (d/b) = 0.05						
0.5	1	0.4432	-0.0151	0.0126	0.1486	0.2921
0.8	1	1.6139	-0.0174	0.0434	0.5293	1.0543
1.0	1	2.5751	-0.0019	0.0817	0.8363	1.6709
0.5	2	0.0244	0.0140	-0.0085	0.0005	0.0259
0.8	2	0.1162	0.0136	-0.0363	0.0053	0.1240
1.0	2	0.2215	0.0033	-0.0652	0.0146	0.2390
0.5	3	0.0085	0.0003	-0.0009	0.0	0.0009
0.8	3	0.0401	-0.0008	-0.0047	0.0002	0.0407
1.0	3	0.0773	-0.0032	-0.0098	-0.0002	0.0789
Thick blade: (d/b) = 0.25						
0.5	1	0.5297	-0.1412	0.0958	0.1841	0.3304
0.8	1	2.0024	-0.1152	0.4240	0.6696	1.1936
1.0	1	3.2908	0.0409	0.7915	1.0606	1.8891
0.5	2	-0.0795	0.0962	-0.0962	-0.0424	-0.0258
0.8	2	-0.3543	0.0030	-0.4333	-0.1662	-0.0850
1.0	2	-0.6645	-0.2125	-0.8171	-0.2799	-0.1220
0.5	3	0.0279	-0.0058	0.0025	0.0054	0.0262
0.8	3	0.0417	-0.0142	0.0187	0.0325	0.1304
1.0	3	0.2801	-0.0207	0.0417	0.0664	0.2531

(b) $\beta_{pc} = 45°$, $\varphi = 0°$, $R = 0$, $\gamma = 30°$

$\frac{\Omega}{\omega_1}$	Mode	All nonlinear terms ignored	Linear Coriolis forces ignored	Nonlinear Coriolis forces ignored	$A_{ijk} = 0$	$D_{ijk} = 0$, $E_{ijk} = 0$
Thin blade: (d/b) = 0.05						
0.5	1	2.5329	-0.1616	0.0548	0.8297	1.6594
0.8	1	11.9310	-0.2295	0.2711	3.5383	7.3843
1.0	1	20.7021	-0.1826	0.5217	5.5451	12.0161
0.5	2	0.1190	0.1290	-0.0417	-0.0010	0.1240
0.8	2	0.6686	0.1879	-0.2135	0.0010	0.7114
1.0	2	1.3752	0.1586	-0.4150	-0.0077	1.4846
0.5	3	0.0406	0.0056	-0.0043	0.0002	0.0413
0.8	3	0.2268	0.0024	-0.0255	-0.0064	0.2322
1.0	3	0.4685	-0.0084	-0.0554	-0.0270	0.4823
Thick blade: (d/b) = 0.25						
0.5	1	2.9356	-1.3250	0.4657	1.0173	1.8434
0.8	1	13.7159	-1.8113	2.3196	4.3004	8.0701
1.0	1	23.7387	-1.2858	4.4403	6.7694	12.9583
0.5	2	-0.3777	1.2557	-0.4620	-0.2114	-0.1264
0.8	2	-1.8834	1.6768	-2.3884	-0.9525	-0.4058
1.0	2	-3.6149	1.1465	-4.7191	1.6652	-0.3663
0.5	3	0.1261	-0.0143	0.0059	0.0218	0.1228
0.8	3	0.7550	-0.0416	0.0816	0.1475	0.7253
1.0	3	1.6052	-0.0644	0.2145	0.3068	1.5186

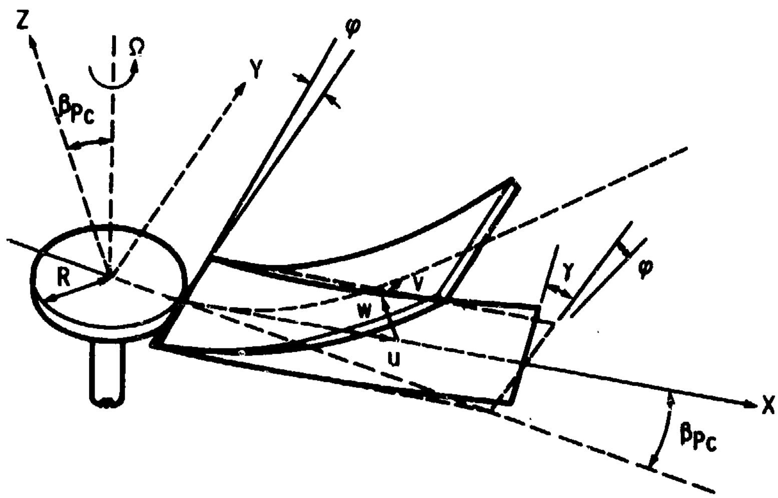

Figure 1. - Blade coordinate system and definition of blade parameters.

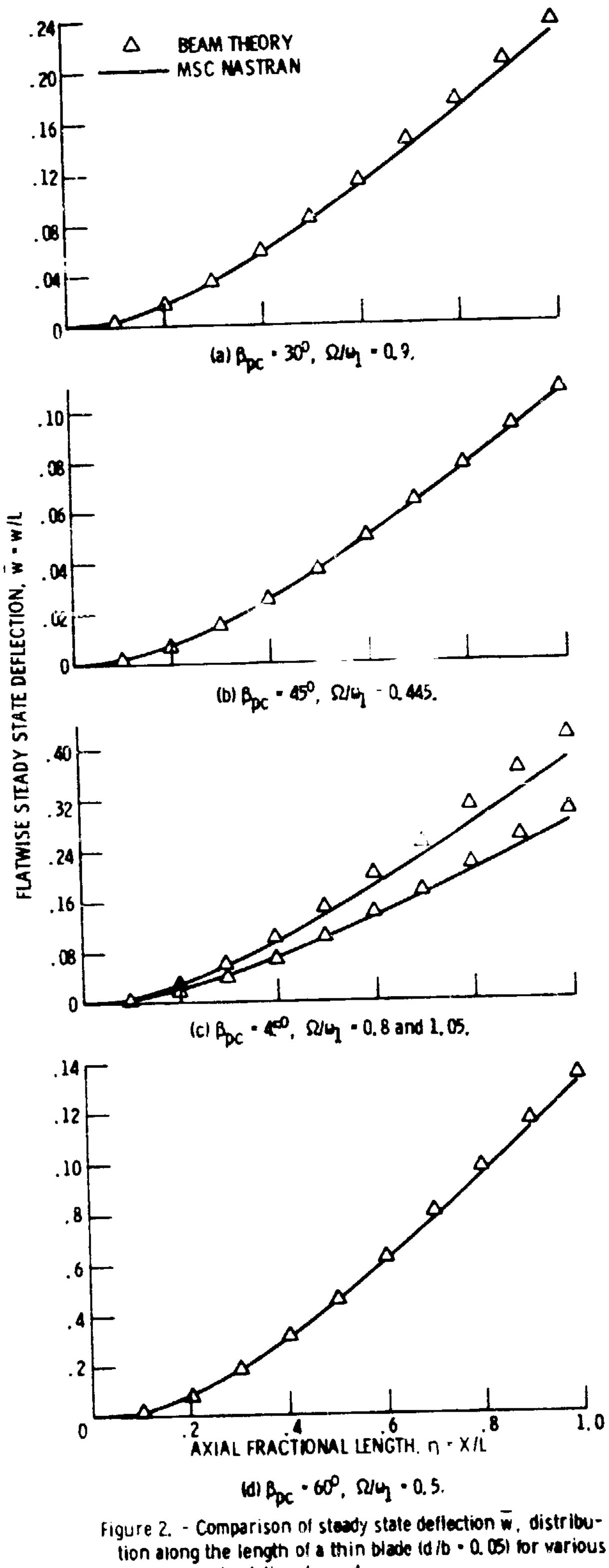

Figure 2. - Comparison of steady state deflection $\bar{w}$, distribution along the length of a thin blade (d/b = 0.05) for various precones and rotational speeds.

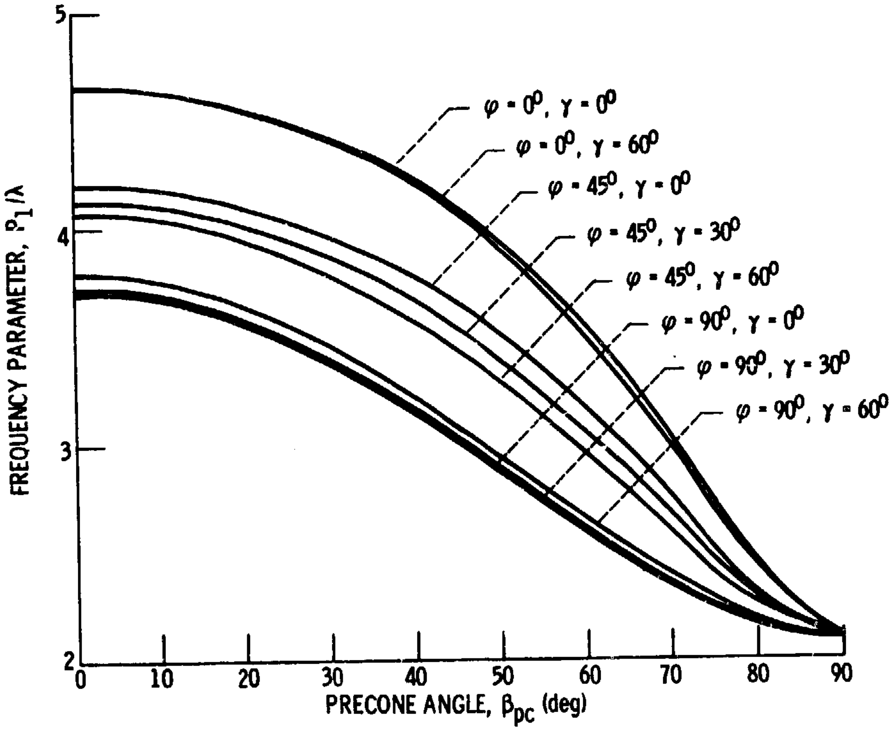

Figure 3. - Effect of pretwist, precone and setting angle variations on the fundamental mode frequency parameter of rotating, thin, blade: Perturbation solution: $d/b = 0.05$, $\Omega/\omega_1 = 0.8$, $L/b = 10$, $L = 5.0$ in.

1. Report No.	2. Government Accession No.	3. Recipient's Catalog No.
NASA TM-87102		

4. Title and Subtitle

Nonlinear Flap-Lag-Extensional Vibrations of Rotating, Pretwisted, Preconed Beams Including Coriolis Effects

5. Report Date

6. Performing Organization Code

505-33-7B

7. Author(s)

K.B. Subrahmanyam and K.R.V. Kaza

8. Performing Organization Report No.

E-2598

10. Work Unit No.

9. Performing Organization Name and Address

National Aeronautics and Space Administration
Lewis Research Center
Cleveland, Ohio 44135

11. Contract or Grant No.

12. Sponsoring Agency Name and Address

National Aeronautics and Space Administration
Washington, D.C. 20546

13. Type of Report and Period Covered

Technical Memorandum

14. Sponsoring Agency Code

15. Supplementary Notes

K.B. Subrahmanyam, on leave from NBKR Institute of Science and Technology, Mechanical Engineering Department, Vidyanagar 524413, India and Research Associate, University of Toledo, Toledo, Ohio 43606; K.R.V. Kaza, NASA Lewis Research Center. Prepared for the 19th Midwestern Mechanics Conference sponsored by the Ohio State University, Columbus, Ohio, September 9-11, 1985.

16. Abstract

The effects of pretwist, precone, setting angle, Coriolis forces and second degree geometric nonlinearities on the natural frequencies, steady state deflections and mode shapes of rotating, torsionally rigid, cantilevered beams are studied in this investigation. The governing coupled equations of flap-lag-extensional motion are derived including the effects of large precone (a component of sweep) and retaining geometric nonlinearities up to second degree. The Galerkin method, with nonrotating normal modes, is used for the solution of both steady state nonlinear equations and linear perturbation equations. Parametric results indicating the individual and collective effects of pretwist, precone, Coriolis forces and second degree geometric nonlinearities on the steady state deflections, natural frequencies and mode shapes of rotating blades are presented and discussed. The results indicate that the second degree geometric nonlinear terms, which vanish for zero precone, can produce frequency changes of engineering significance (of the order of 20 percent on the fundamental mode, and about ± 4 percent on the second mode). Further confirmation of the validity of including second degree nonlinearities in the analysis is achieved by comparisons of beam theory results to those generated by MSC NASTRAN. The results further indicate that the linear and nonlinear Coriolis effects must be included in analyzing thick blades while these effects can be neglected in analyzing thin blades, typical of advanced turboprop blade configurations. The Coriolis effects are significant on the first flatwise and the first edgewise modes, but are insignificant on higher modes. For those modes where the effect is significant, the linear and nonlinear Coriolis effects oppose one another, the nonlinear effects generally being stronger.

17. Key Words (Suggested by Author(s))	18. Distribution Statement
Nonlinear differential equations; Coupled vibration; Rotation; Pretwist; Precone; Coriolis effects; Second degree geometric nonlinearities	Unclassified - unlimited STAR Category 39

19. Security Classif. (of this report)	20. Security Classif. (of this page)	21. No. of pages	22. Price*
Unclassified	Unclassified		

*For sale by the National Technical Information Service, Springfield, Virginia 22161